Coulomb Lindhard approximation: Nonlinear excitation effects for fast ions penetrating a free-electron gas

J. E. Miraglia

Instituto de Astronomía y Física del Espacio, Consejo Nacional de Investigaciones Científicas y Técnicas, Departamento de Física, Facultad de Ciencias Exactas y Naturales, Universidad de Buenos Aires, Casilla de Correo 67, Sucursal 28, 1428 Buenos Aires, Argentina

(Received 25 April 2003; published 29 August 2003)

We introduce a distorted wave method to calculate the nonlinear excitation effects occurring when a fast bare ion penetrates a free-electron gas. The central scheme of this work is to replace the undistorted plane waves leading to the Lindhard dielectric response function (or random phase approximation) by Coulomb waves with an effective charge. This impulse-type approximation is valid for velocities larger than the Fermi velocity. Stopping and mean free path are presented for impact of bare multicharged ions on aluminum free-electron gas. The Barkas effect is theoretically found, i.e., negative heavy particles lose energy at the lower rate than positive particles of the same velocity do. As the projectile charge increases, the single differential cross section per unit energy presents two effects: the plasmon peak sharpens and the binary peak starts to be increasingly noticeable.

DOI: 10.1103/PhysRevA.68.022904 PACS number(s): 34.50.Bw

I. INTRODUCTION

As a heavy particle penetrates a free-electron gas (FEG), it gives rise to binary as well as collective-oscillations (plasmons) excitations. A huge amount of literature has been devoted to the calculation of the linear response; i.e., the first order in the projectile charge Z_P originally developed by Lindhard [1]. After the Barkas effect was found [2], some efforts have been focused on the calculation of the nonlinear effects [3]. Such theories can be classified, to our understanding, into four major lines; viz., (i) the hydrodynamic models [4–6], (ii) the oscillator model [7], (iii) the binary scattering method [8,10], and (iv) the perturbative expansion [11–17].

The hydrodynamic as well as the oscillator models are very appealing. With them higher orders in Z_P can be calculated after some feasible numerical calculations. In spite of a great deal of physical visualizations, the main doubt rests on the validity of such models to represent the details of the real quantum process. The binary scattering method is certainly an appropriate model to treat stopping power for impact velocities v less that the Fermi velocity k_F of the FEG [11]. However, for a reason that is not very well understood, this model still produces a notable performance when compared with the experiments for $v > k_F$, even though it lacks collective oscillations [10]. It is well known that collective excitations provide nearly half of the stopping power at high impact velocities (equipartition rule) and such processes are not contained in the binary scattering method. Undoubtedly, the perturbative expansion is a good starting approach to face the problem, however, after tedious numerical calculation only it is possible to calculate the first correction to the Lindhard dielectric function in terms of Z_P. Moreover, its range of validity is not sufficient to predict quantitatively the experiments of protons ($Z_P=1$) [18] and antiprotons ($Z_P=-1$) impact [19] at $v \approx k_F$.

In this paper we attempt a different approach based on the application of the distorted wave methods, commonly used in the theory of inelastic atomic collisions [20]. The essential idea is to start from the formal definition of the dielectric function, for example, from the one developed by Ritchie [21], and replace the induced electronic density calculated with plane waves by the one obtained with Coulomb waves with an effective charge. This model includes *all* the perturbative orders, at least in an approximate way. We call this model the Coulomb Lindhard approximation (CLA). It is a typical impulse approximation, which attempts to describe a many-body quantum problem in terms of known two-body scattering wave functions [20]. As in the classical counterpart, the basic assumption of the impulse approximation is that the dynamics of the correlations does not play an important role during the collision, and it happens when $v \gg k_F$.

In Sec. II we present the theory and in Sec. III the results. Atomic units are used.

II. THEORY

Let us consider a projectile of charge Z_P moving inside a FEG. The electrons feel the interaction of the projectile as well as that of the rest of the electrons conforming a self-consistent potential $V(\mathbf{r})$ which induces an electron density. Such an electron density in the projectile frame is defined in the usual way, $\rho_{\mathbf{K}}(\mathbf{r}) = |\Phi^+_{\mathbf{K}}(\mathbf{r})|^2$ where $\mathbf{K}=\mathbf{k}-\mathbf{v}$ is the relative electron momentum with respect to the projectile, $\mathbf{k}$ is the momentum of the electron with respect to the solid frame, $\mathbf{v}$ is the ion velocity, and $\Phi^+_{\mathbf{K}}(\mathbf{r})$ is the exact continuum wave function of the electron in the full self-consistent unrestrained field $V(\mathbf{r})$ [21]. The Coulomb Lindhard approximation, here proposed, consists in approximating the unknown state $\Phi^+_{\mathbf{K}}(\mathbf{r})$ by a continuum function of the Schrödinder equation in the Coulomb potential $V_C(\mathbf{r}) = -Z_C/r$. Such a Coulomb continuum function $\Psi^+_{\mathbf{K}}(\mathbf{r})$ reads

$$\Psi^+_{\mathbf{K}}(\mathbf{r}) = \psi_{\mathbf{K}}(\mathbf{r}) N_{K1} F_1(ia,1,iK\eta), \quad \eta = r - \hat{\mathbf{K}}\cdot\mathbf{r}, \quad (1)$$

where

$$N_K=\exp(a\pi/2)\Gamma(1-ia),\quad \psi_{\mathbf{K}}(\mathbf{r})=\frac{\exp(i\mathbf{K}\cdot\mathbf{r})}{(2\pi)^{3/2}},\quad (2)$$

$a=Z_C/K$ is the Coulomb parameter, and Z_C is an effective Coulomb charge whose expression will be defined later in Sec. II B. The integral representation of the Fourier transform of the Coulomb density reads

$$\begin{aligned}\tilde{\rho}_{\mathbf{K}}(\mathbf{q})&=\int d\mathbf{r}\frac{\exp(-i\mathbf{q}\cdot\mathbf{r})}{(2\pi)^{3/2}}\rho_{\mathbf{K}}(\mathbf{r})\\&=\frac{|N_K|^2}{(2\pi)^{9/2}}\int d\mathbf{r}\exp[-i\lambda r-i\mathbf{q}\cdot\mathbf{r}-iK\eta]\\&\quad\times{}_1F_1(1+ia,1,iK\eta)\,{}_1F_1(ia,1,iK\eta),\end{aligned}\quad (3)$$

where we have used the Kummer transformation, and $\lambda\to0^+$. After lengthy algebra involving Nordsieck integrals [22,23], we obtain

$$\tilde{\rho}_{\mathbf{K}}(\mathbf{q})=\frac{1}{(2\pi)^{3/2}}[C\Delta_1\delta(\mathbf{q})-C\Delta_2\tilde{V}_C(\mathbf{q})],\quad (4)$$

where

$$\tilde{V}_C(\mathbf{q})=-\sqrt{\frac{2}{\pi}}\frac{Z_C}{\lambda^2+q^2},\quad (5)$$

is the Fourier transform of $V_C(\mathbf{r})$,

$$A_\pm=-\frac{2}{g_0^\pm d},\quad C=|N_K|^2(A^+)^{-2ia},\quad d=\lambda^2+q^2,\quad (6)$$

$$g_0^\pm=\left[\frac{1}{2}k^2-\frac{1}{2}(\mathbf{q}\pm\mathbf{k})^2\pm(\omega+i\lambda)\right]^{-1},\quad (7)$$

$$\Delta_1=G_1(1+2ia)+G_2ia(1+ia)\left(\frac{g_0^+}{g_0^-}-1\right),\quad (8)$$

$$\Delta_2=N^+g_0^++N^-g_0^-,\quad (9)$$

$$N^+=G_2(1+ia),\quad N^-=N^++2G_3,\quad (10)$$

$$G_1={}_2F_1(1-ia,-ia,1,X),\quad (11)$$

$$G_2={}_2F_1(1-ia,-ia,2,X),\quad (12)$$

$$G_3=G_1-(1+ia)G_2=-ia\,{}_2F_1(1-ia,1-ia,2,X),\quad (13)$$

and $X=1-A_+A_-$. It can be proved that if $\mathbf{q}=0$, then $C\Delta_1=1+O(\lambda)$. It implies that the first term in Eq. (4) normalizes properly to the Dirac delta.

If $\tilde{\rho}_{\mathbf{K}}(\mathbf{q})$ were expanded in a perturbative series in power of $\tilde{V}_C(\mathbf{q})$, we would obtain the first order

$$\tilde{\rho}_{\mathbf{K}}(\mathbf{q})=\frac{1}{(2\pi)^{3/2}}[\delta(\mathbf{q})-(g_0^++g_0^-)\tilde{V}_C(\mathbf{q})].\quad (14)$$

By setting $\widetilde{V_C}(\mathbf{q})=\tilde{V}(\mathbf{q})$ in Eq. (14) we obtain the expression of the density leading to the Lindhard dielectric function.

The first element of Eq. (4) can be dropped since it does not involve transitions ($q=0$); it just compensates the background of positive charges. Replacing the density given by Eq. (4) in the basic equation defining the dielectric function $\varepsilon(\mathbf{q})$ (for instance, Eq. (2.8) of Ref. [21]], and adding on all possible states of the FEG, one obtains

$$[\varepsilon(\mathbf{q})-1]\tilde{V}(\mathbf{q})=\frac{4\pi}{q^2}2\int\frac{d\mathbf{k}}{(2\pi)^3}\tilde{\rho}_{\mathbf{K}}(\mathbf{q})\quad (15)$$

$$=-\tilde{V}_C(\mathbf{q})\frac{4\pi}{q^2}\frac{2}{(2\pi)^{9/2}}\int d\mathbf{k}C\Delta_2,\quad (16)$$

where $\Theta=\Theta(k_F-k)$ and $\tilde{V}(\mathbf{q})$ is the self-consistent potential.

The central point of this approximation is to choose $Z_C=Z_C(Z_P,\mathbf{q})$ so that we can invoke self-consistency by asserting $\tilde{V}_C(\mathbf{q})\cong\tilde{V}(\mathbf{q})$. We will return later to this point in Sec. II B. By invoking this identity, we can write the CLA response function ε_{CL} as

$$\varepsilon_{CL}(q,\omega)=1-\frac{4\pi}{q^2}2\int\frac{d\mathbf{k}}{(2\pi)^3}\Theta[\mathcal{G}^+\Theta^++\mathcal{G}^-\Theta^-],\quad (17)$$

where the 2 in front of the integral accounts for the two states of the spins, $\Theta^\pm=\Theta(|\mathbf{q}\pm\mathbf{k}|-k_F)$, $\omega=\mathbf{q}\cdot\mathbf{v}$, and

$$\mathcal{G}^+=CN^+g_0^+,\quad \mathcal{G}^-=CN^-g_0^-.\quad (18)$$

Equation (17) is the central finding of this work.

We should stress that the approximation developed here is a nonlinear model. One could expand $1/\varepsilon_{CL}(q,\omega)$ in an infinite series in terms of Z_P, to give

$$\frac{1}{\varepsilon_{CL}(q,\omega)}=\frac{1}{\varepsilon_L(q,\omega)}+\sum_{j=1}^{\infty}\frac{Z_P^j}{\varepsilon^{(j)}(q,\omega,v)}.\quad (19)$$

The first element $1/\varepsilon_L(q,\omega)$ is the linear Lindhard term. The next term, $j=1$, is an approximation to the nonlinear contribution developed in recent papers [11,13–17], and so on. Performing this expansion is no easy task, since we have to differentiate the hypergeometric function ${}_2F_1$ with respect to the parameter a, producing nonstandard functions which are not easy to work with.

As the Coulomb charge vanishes, $Z_C\to0$, or $v\to\infty$, $a=Z_C/|\mathbf{k}-\mathbf{v}|\to0$, we have from Eq. (17) $G_{1,2}\to1$, $N^\pm\to1$, $|N_K|\to1$, $C\to1$, $\mathcal{G}^\pm\to g_0^\pm$ and so the usual Lindhard dielectric function ε_L is recovered

$$\varepsilon_L(q,\omega)=1-\frac{4\pi}{q^2}2\int\frac{d\mathbf{k}}{(2\pi)^3}\Theta[g_0^+\Theta^++g_0^-\Theta^-].\quad (20)$$

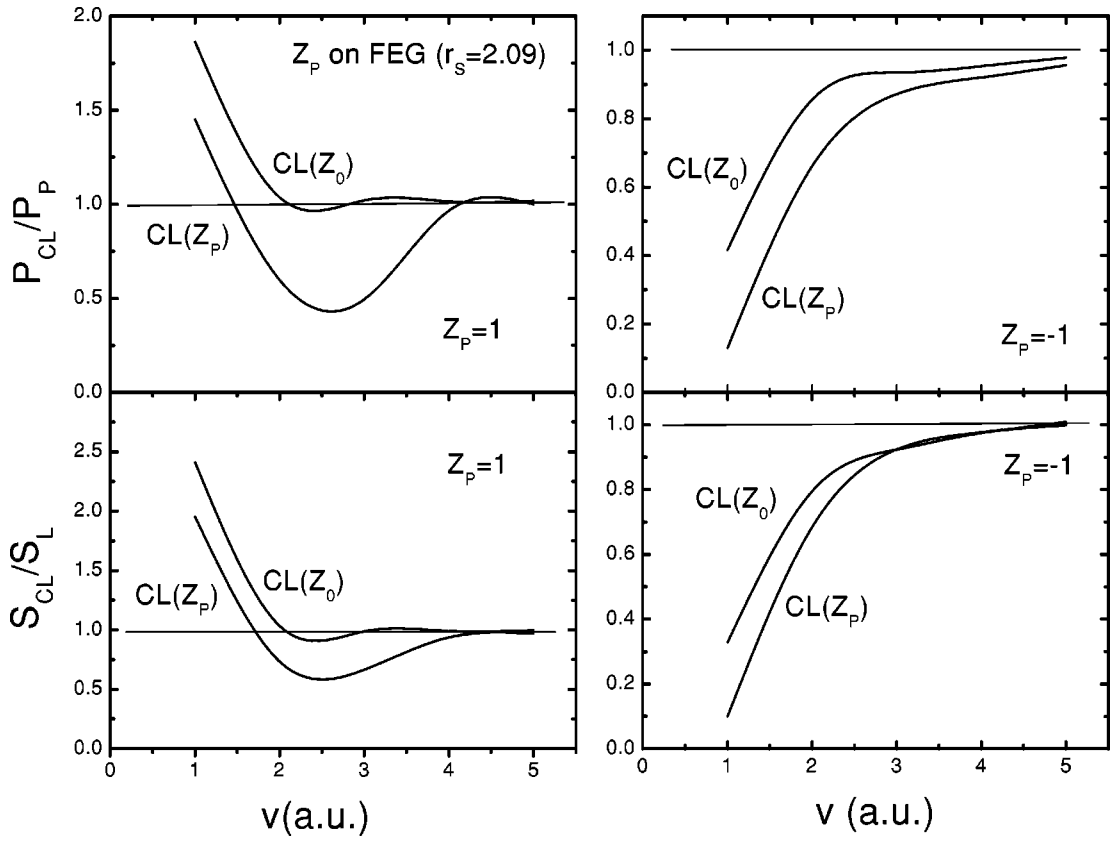

FIG. 1. Ratio of the probability and stopping calculated with the Coulomb-Lindhard approximation to the first-order Lindhard as a function of the impact velocity for two different values of the effective Coulomb charge $Z_C=Z_P$ and $Z_C=Z_0$ as indicated. The target is a free-electron gas with $r_S=2.09$ (aluminum case) and the projectiles are protons ($Z_P=1$) and antiprotons ($Z_p=-1$) as indicated. The validity of the theory should hold for $v>2$.

Therefore, no mater which Z_C we choose, the first order of $\varepsilon_{CL}(q,\omega)$ is always self-consistent and it coincides with the one of Lindhard.

A. A practical expression

The argument of the hypergeometric functions ${}_2F_1$ can take values larger than unity. Evaluation in these points is complicated since the usual analytical continuation for large values of X cannot be used because the argument of the γ functions is zero [see, for example, Eq. (15.3.7) of Ref. [24]]. In this case, it is more convenient to change the argument of the hypergeometric function from X to Y, where $Y=X/(X-1)$. After some algebra not shown here, the dielectric function $\varepsilon_{CL}(q,\omega)$ is found to keep the same form of Eq. (17), where now

$$\mathcal{G}^{\pm}=[N_K^* A_-^{+ia}][\mathcal{K}^{\pm} g_0^{\pm}][A_+^{-ia} N_K], \tag{21}$$

and the kernels $\mathcal{K}^{\pm}$ read

$$\mathcal{K}^{+}=(1+ia)_2F_1(1+ia,-ia,2,Y), \tag{22}$$

$$\mathcal{K}^{-}=2_2F_1(ia,-ia,1,Y)-\mathcal{K}^{+}. \tag{23}$$

At the very end, we conclude that $\varepsilon_{CL}(q,\omega)$ is derived from $\varepsilon_L(q,\omega)$ by replacing $g_0^{\pm}$ by $\mathcal{G}^{\pm}$. It is the representation of the propagator $\mathcal{G}^{\pm}$, the one that contains the Coulomb potential to all orders. For any other potential it is quite possible that the structure of the dielectric response function remains the same. The mathematical form of the propagator given by Eq. (21) is very common in the theory of atomic collision when distorted wave methods are used [25].

B. The Coulomb charge

The use of Coulomb waves lets us handle the algebra to be written down in suitable closed form, but the real interaction is not Coulombic but screened due to the reaction of the electron gas. We cast on Z_C the responsibility to accomplish the self-consistency when $\widetilde{V_C}(\mathbf{q})\cong\widetilde{V}(\mathbf{q})$ was invoked. The toughest (and unrealistic) approximation would be the chosen $Z_C=Z_P$, i.e., where the interactions with the rest of the electrons are fully neglected.

To include the interaction with the other electrons, one may resort to an iterative scheme by starting with $Z_C=Z_P/\varepsilon_L(q,\omega)$. But this is not an appropriate charge in our scheme, since it has an imaginary component and so the wave function vanishes at infinity [26]. It implies that it does not provide the correct asymptotic behavior. Then Z_C must be real and so it should depends only on q (spherical symmetry). It seemed to us more convenient to use the so-called static potential, i.e., $Z_C=Z_0$, where

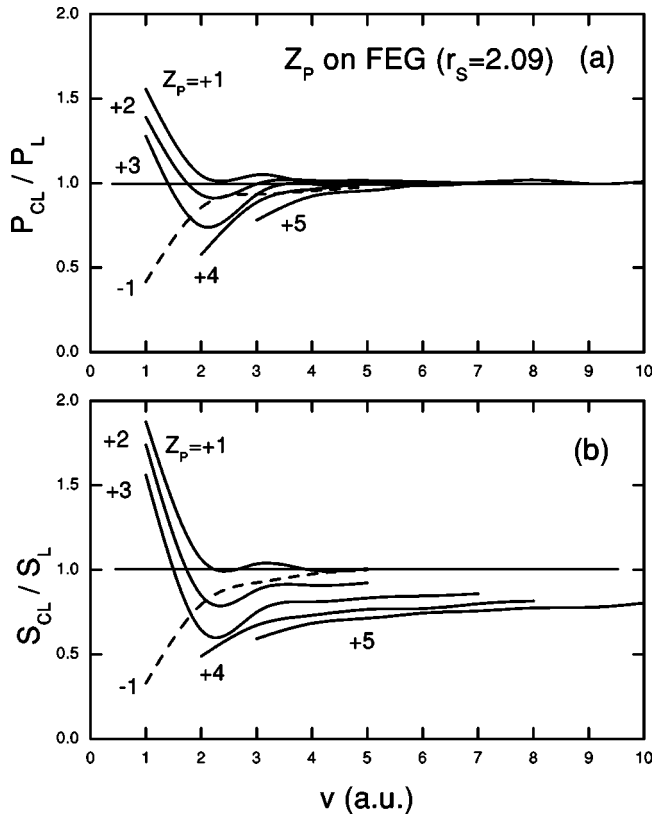

FIG. 2. (a) Ratio of the probability of inelastic transitions calculated with the Coulomb-Lindhard approximation to the first-order Lindhard as a function of the impact velocity for different Coulomb projectile charges, as indicated. The target is a free-electron gas with $r_S=2.09$ (aluminum case). The validity of the theory should hold for $v>2$. (b) Similar to (a) for the stopping.

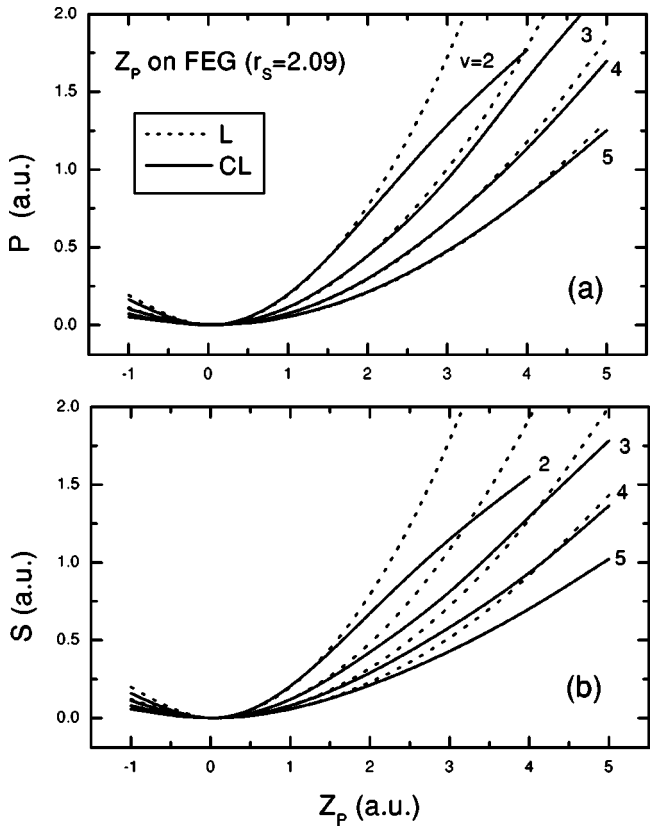

FIG. 3. (a) Probability per unit length of inelastic transitions as a function of the projectile Coulomb charge for different velocities, as indicated. The target is a free-electron gas with $r_S=2.09$ (aluminum case). Notation: solid lines, the Coulomb-Lindhard approximation and dotted lines, the first-order Lindhard result. (b) Similar to (a) for the stopping.

$$Z_0=Z_P Re\left[\frac{1}{\varepsilon_L(q,0)}\right]\rightarrow\begin{cases}Z_P & \text{as} \quad q\rightarrow\infty\\ 0 & \text{as} \quad q\rightarrow 0,\end{cases} \tag{24}$$

which ensures the Coulomb potential at short distances, $r\rightarrow 0$ (or $q\rightarrow\infty$), and Fridel oscillations at large distances $r\rightarrow\infty$ (or $q\rightarrow 0$).

We have explored several other alternatives, such as the Yukawa potential $Z_C=q^2/(q^2+\zeta^2)$, with $\zeta^2=\omega_P^2/(v^2+k_F^2/3)$ [27], the Fourier transform of the Nagy and Echenique potential [10], etc. All these results are found to be in between $Z_C=Z_P$ and $Z_C=Z_0$. Dependence of the stopping with Z_C will be presented in Fig. 1 below. Two observations should be noted.

First, selecting $Z_C=Z_0$ as given by Eq. (24) does *not* mean that we are considering the wave function of the full static potential (which has no closed form whatsoever) but we are only using an effective Coulomb charge so that it has the same Fourier transform of the potential.

Second, one should not forget that we are considering a projectile with a *bare* punctual Coulomb charge Z_P (here called the seed) shielded by the factor $\mathrm{Re}[1/\varepsilon_L(q,0)]$ which represents the enhancement of the electronic density of the FEG accompanying the projectile. However, it is well known that within the solid, the projectile captures and loses electrons to give rise to different charge states. If this is the case, we can no longer use Z_P as the seed charge. One could extend the present model by incorporating the projectile electrons. For example, the seed charge may be changed from $Z_P\rightarrow Z_{PN}-\Sigma_{j=1}^{n_P}\langle\varphi_j|\exp(i\mathbf{q}\cdot\mathbf{r})|\varphi_j\rangle$, where Z_{PN} is the projectile nuclear charge, n_P is the number of electrons and φ_j is the wave function of the bound electrons. Also it could be possible to tackle the problem projectiles with structured [28].

One can prove that the screening of the Coulomb potential is proportional to r_S^{-x} (r_S is the Seitz radio). If we consider the screening ζ, for example, x ranges from 1/2 to 3/2 depending on v. Therefore, as $r_S\rightarrow 0$ (high density limit), $\zeta\rightarrow\infty, Z_C\sim 0$, and so the plane wave is a good representation and the Lindhard linear response holds quite well. On the contrary, as $r_S\rightarrow\infty$ (low-density limit), $\zeta\rightarrow 0, Z_C\sim Z_P$, and so large correction is expected. This qualitatively estimation is in agreement with previous findings [11,14].

III. RESULTS

A three-dimensional integral on $\mathbf{k}$ is required to obtain $\varepsilon_{CL}(q,\omega)$ from [Eq. (17)]. Two further integrals on q and ω are involved in the calculation of

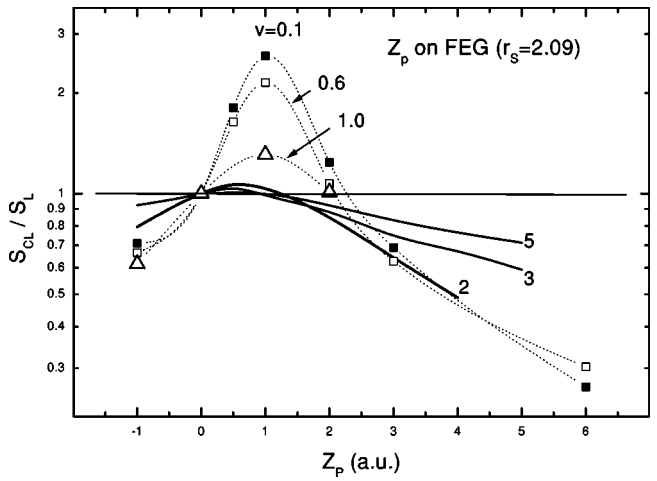

FIG. 4. Ratio of the stopping to the first-order Lindhard as a function of the projectile Coulomb charge for different impact velocities, as indicated. The target is a free-electron gas with $r_S=2.09$ (aluminum case). Impact velocities $v=0.1$ (full squares) and 0.6 (empty squares) are the results of Salin *et al.* using the DFT [27]. The values for $v=1$ (triangles) correspond to the *estimated* experiments [31] for protons and antiprotons on aluminum along with the theoretical results of α particles impact [32]. The solid lines are the results using the Coulomb-Lindhard approximation calculated for integer Coulomb charges and $Z_P=0.5$. The interpolated lines are just to help visualization.

$$P_j^{(n)}=S_0\int_0^\infty d\omega\omega^n\int_{\omega/v}^\infty\frac{dq}{q}\mathrm{Im}\left[\frac{1}{\varepsilon_j(q,\omega,Z_0)}\right], \qquad (25)$$

with $S_0=-2Z_P^2/(\pi v^2)$, to obtain the stopping $S=P^{(1)}$, or the probability (the inverse of the mean free path) $P=P^{(0)}$, per unit path length. The subindexes $j=CL$ and L will be used to denote the calculation with our CLA and the Lindhard first order, respectively. The numerical calculation of the CLA approximation is very difficult since the integrand involves the hypergeometric function ${}_2F_1$ which in some cases has to be evaluated by solving its differential equation. Two weeks of CPU time in a cluster of 4 PC of 1.6 GHz each have been required to obtain the results here presented. To calculate the integrations, an adaptive numerical code has been used with a relative error less than 1%. Still we have found some regions where the obtained curves do not have the optimal smoothness. We have found the same pathology of the second-order dielectric formalism [17]: for $Z_P<0$, the probability was found to be slightly negative in a region at high values of ω, where the contribution to the integrated value is rather negligible. Anyway, as in Ref. [17], we have replaced such negative values by zero. The first-order Lindhard results were calculated from Eq. (20) in the same way, i.e., with the five-dimensional numerical integral.

We will focus on a FEG characterized by $r_S=2.09$ ($k_F=0.92,\omega_p=0.566$) and $\lambda=0.0375$, which corresponds to the conducting electrons of aluminum. Integer values of the charge Z_P ranging from -1 to 5 (and also $Z_P=0.5$), and integer values of the velocity v from 1 to 10 were considered. In all cases we expect the results to be valid for $v\gg k_F$, say $v>2$.

In Fig. 1, we plot the ratio between the Coulomb-Lindhard and the Lindhard results for the probability and stopping of protons and antiprotons on aluminum FEG for two different values of the Coulomb charges $Z_C=Z_P$ and $Z_C=Z_0$ as given by Eq. (24). Although differences are observed, the same qualitative behaviors are present. For example, in both cases the Barkas effect is clearly spotted (stopping of protons are larger than antiprotons). Although we include results for $v=1$, it is important to recall that CL values are expected to be valid, at least, for $v>2$. From now on we will concentrate on the use of $Z_C=Z_0$.

In Fig. 2, we plot the ratio between the Coulomb-Lindhard and the Lindhard results for the probability and stopping of different projectile charges as a function of the impact velocity. Some oscillations are observed for the first positive charges. For the stopping the convergence to unity at large velocities decreases with the projectile charge.

Figure 3 shows the absolute values of the probability and stopping along with the Lindhard ones that are proportional to Z_P^2. The CLA departures from this tendency. It produces a saturation effect, i.e., the results seem to tend to a constant. The departure from the Z_P^2 law depends on the velocity; the larger the velocity, the larger the charge where departure occurs. This behavior with Z_P is similar to the one found in ion-atom excitation and ionization [30], and perhaps the same physics is involved. One can then expect that, as in the ionization case, saturation starts for $Z_P\sim v$. The saturation is a consequence of the *infinite* series in terms of Z_P. If we kept the first correction ($j=1$) in Eq. (19) the probabilities as well as the stopping would diverge as Z_P^3.

In Fig. 4 we compare our results with the ones reported by Salin *et al.* [29] by plotting the ratio S_{CL}/S_L as a function of Z_P. These authors have used a very refined method. They employed the density-functional theory (DFT) to describe the electron density, and so the corresponding induced potential was derived. This potential (with cylindric symmetry) was expanded in harmonic spherics solving the equations for each angular orbital. This method holds for small velocities, $v<k_F$, because both, the DFT cannot describe the kinetics at high energies and the collisional model used does not account for collective oscillation (plasmons), which for protons on aluminum starts at 40 keV ($v=1.3$). The CLA seems to continue reasonably the tendency from low velocity ($v=0.1$–0.8 a.u.) to the high velocity region ($v>2$). In the high velocity limit, we expect the ratio to tend to the unity, i.e., $S_{CL}/S_L\to 1$ as $v\to\infty$. Just to show the link between the DFT (valid for $v\ll k_F$) and our CLA (valid for $v\gg k_F$), we show for $v=1\simeq k_F=0.92$ a curve interpolated by the estimated experiment [31] for antiproton ($Z_P=-1$) and protons ($Z_P=1$) from Refs. [18] and [19], and the theoretical result for α particles impact ($Z_P=2$) [32].

Figure 5 shows the single differential cross section for multicharged bare ions on aluminum FEG at $v=3$ a.u. as a function of the projectile energy loss ω. For low projectile charges ($Z_P=1$), the spectra show a single peak near the plasmon energy ($\omega\sim 0.6$). To understand the mechanism involved in this structure, it is convenient to extract the binary contribution from the total value which includes also the

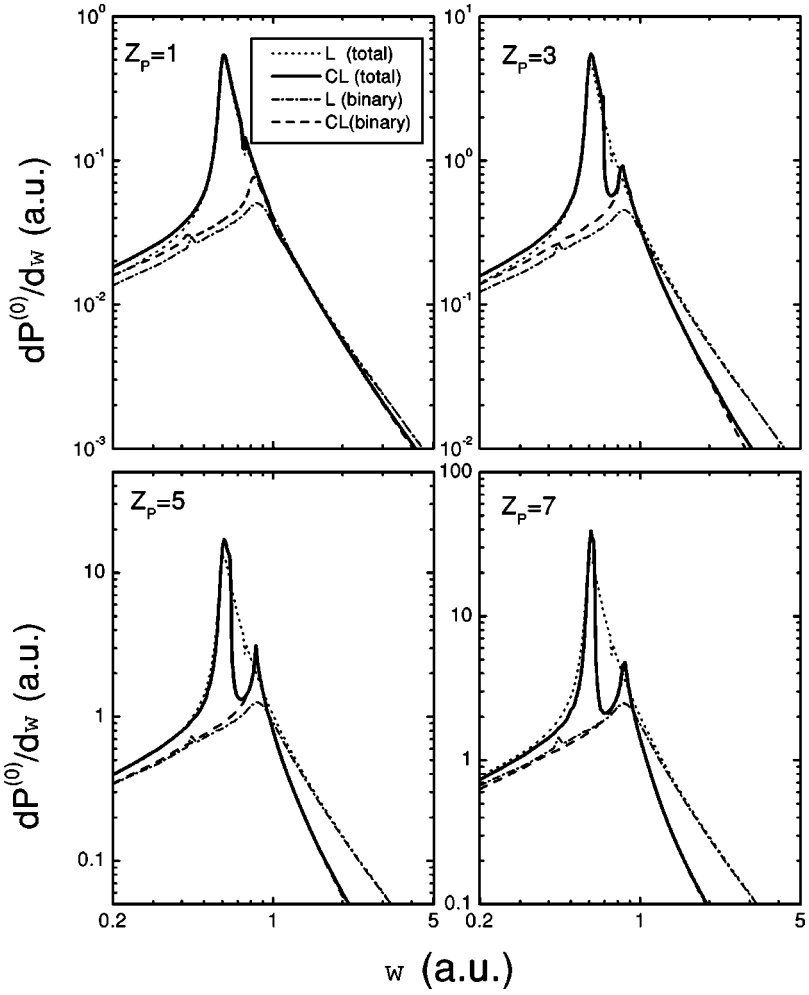

FIG. 5. Projectile energy loss distributions for different projectile charges as indicated for $v=3$. The target is a free-electron gas with $r_S=2.09$ (aluminum case). Notation: solid (dashed) lines, the full (binary alone) contribution of the Coulomb-Lindhard approximation; dotted (dash-dotted) lines, the full (binary alone) contribution of the Lindhard first order.

collective excitations. The binary contribution can be estimated simply by inserting the step function

$$\Theta(q^2k_F^2-(\omega-q^2/2)^2), \tag{26}$$

in the integrand of Eq. (25). This factor reduces the integration to the region where energy and momentum are conserved in a collision with a single electron. Binary contributions to the probability are included in Fig. 5 for Lindhard (dot-dashed lines) and Coulomb-Lindhard (dotted lines) approximations. As Z_P increases two effects can be observed: the plasmon peak at $\omega\sim 0.6$ sharpens and the binary peak at $\omega\sim 0.85$ starts to be increasingly noticeable. Possibly, it could be explained as a two-or-more step processes including a plasmon as an intermediate state. Even though both (binary and collective) peaks sharpen, we have found that the equipartition rule still holds within numerical uncertainties. It is interesting to study the dependence of these structures on the projectile charge as shown in Fig. 6. The enhancement of the binary peak only occurs for large positive charges but it is not present for large (and unrealistic) negative charge. The physical interpretation may be found in the fact that positive charges attract the electrons and forces them to collide with it

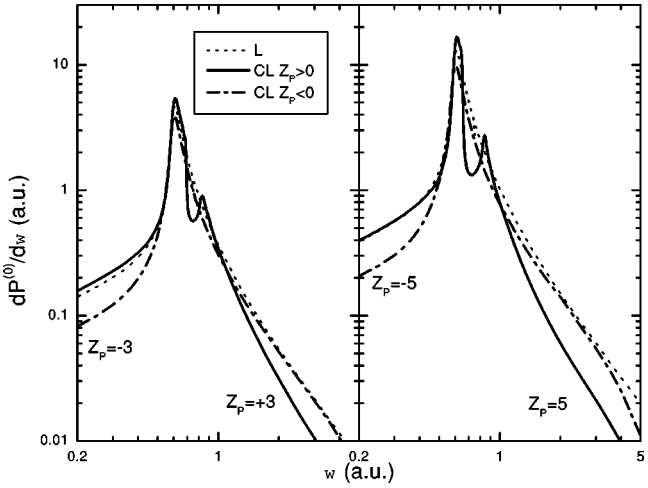

FIG. 6. Projectile energy loss distributions for different projectile charges as indicated for $v=3$. The target is a free-electron gas with $r_S=2.09$ (aluminum case). Notation: solid lines (dot-dashed), the full contribution of the Coulomb-Lindhard approximation for positive (negative) projectile charge and dotted lines, the first-order Lindhard term.

in the next step, while negative charges repel the electrons and so no further collisions take place. These findings are present only in a nonperturbative model since it necessarily involves high perturbative orders.

In conclusion we have developed a distorted wave model based on the impulse approximation to calculate the nonlinear effects (including all the order in Z_P) when a heavy projectile penetrates a FEG. The method should be reliable for large velocity impact, i.e., for $v \gg k_F$, and includes not only the plasmon and binary excitations separately but also the processes involving the mixture of both types of excitations. It complements the binary scattering model [8,9] valid for $v \ll k_F$, where collective oscillations are absent, and extends the range of validity of the perturbation theory [11,13–17] for $v \gg k_F$.

ACKNOWLEDGMENTS

I would like to thank M.S. Gravielle and D.G. Arbó for the important contributions to the present theory. The support of the Grant Nos. UBACyT X044, PICT99 0306249, and PICT98 0303579 is acknowledged.

[1] J. Lindhard, K. Dans. Vidensk. Selsk. Mat. Fys. Medd. **28**, 8 (1954).
[2] W.H. Barkas, J.W. Dyer and H.H. Heckman, Phys. Rev. Lett. **11**, 26 (1963).
[3] J.C. Asley and R.H. Ritchie, Phys. Status Solidi **38**, 425 (1970).
[4] R. Kronig and J. Korringa, Physica (Amsterdam) **10**, 406 (1943).
[5] J.J. Dorado, Oakley H. Crawford, and Fernando Flores, Nucl. Instrum. Methods Phys. Res. B **93**, 175 (1994).
[6] A. Arnau and E. Zaremba, Nucl. Instrum. Methods Phys. Res. B **90**, 32 (1994).
[7] H.H. Mikkelsen and P. Sigmund, Phys. Rev. A **40**, 101 (1989).
[8] P. Sigmund, Phys. Rev. A **26**, 2497 (1982).
[9] N. R. Arista, Nucl. Instrum Methods Phys. Res. B (unpublished).
[10] I. Nagy and P.M. Echenique, Phys. Rev. A **47**, 3050 (1993).
[11] C.D. Hu and E. Zaremba, Phys. Rev. B **37**, 9268 (1988).
[12] H. Esenben and P. Sigmund, Ann. Phys. (N.Y.) **201**, 152 (1990).
[13] J.M. Pitarke, R.H. Ritchie, P. Echenique, and E. Zaremba, Europhys. Lett. **24**, 613 (1993).
[14] J.M. Pitarke, R.H. Ritchie, and P.M. Echenique, Phys. Rev. B **52**, 13 883 (1995).
[15] A. Bergara, I. Campillo, J.M. Pitarke, and P.M. Echenique, Phys. Rev. B **56**, 15 654 (1997).
[16] D.G. Arbó, M.S. Gravielle, and J.E. Miraglia, Phys. Rev. A **62**, 032901 (2000).
[17] D.G. Arbó, M.S. Gravielle, and J.E. Miraglia, Phys. Rev. A **64**, 022902 (2001).
[18] J.H. Ormrod and H.E. Duckworth, Can. J. Phys. **41**, 1424 (1963); J.H. Ormrod, J.R. MacDonald, and H.E. Duckworth, *ibid.* **43**, 275 (1965); W. White, J. Appl. Phys. **38**, 3660 (1967); S. Kreusler, C. Varelas, and R. Sizmann, Phys. Rev. B **26**, 6099 (1982).
[19] S.P. Møller *et al.*, Phys. Rev. A **56**, 2930 (1997).
[20] J.P. Coleman, *Case Studies in Atomic Collision Physics*, edited by E.W. McDaniel and M.R.C. McDowell (North-Holland, Amsterdam, 1969), Vol. I, Chap. 3, and references within.
[21] R.H. Ritchie, Phys. Rev. **114**, 644 (1959).
[22] A. Nordsieck, Phys. Rev. **93**, 785 (1954).
[23] M.S. Gravielle and J.E. Miraglia, Comput. Phys. Commun. **69**, 53 (1992).
[24] M. Abramowitz and I. Stegun, *Handbook of Mathematical Functions* (Dover, New York, 1972), Chap. 15.
[25] J.E. Miraglia, J. Phys. B **15**, 4205 (1982).
[26] For large distances, $\Psi^+_{\mathbf{K}}(\mathbf{r}) \to \psi_{\mathbf{K}}(\mathbf{r}) \exp[-ia \ln(2k\eta)]$. If Z_0 (and so a) is complex, $|\Psi^+_{\mathbf{K}}(\mathbf{r})|$ will asymptotically diverge or vanish depending on the sign of its imaginary part.
[27] D. Arbó and J.E. Miraglia, Phys. Rev. A **58**, 2970 (1998), Ref. [20].
[28] Zeev Vager and Donald S. Gemmell, Phys. Rev. Lett. **37**, 1352 (1976).
[29] A. Salin, A. Arnau, P.M. Echenique, and E. Zaremba, Phys. Rev. B **59**, 2537 (1999).
[30] C.O. Reinhold, C.A. Falcón, and J.E. Miraglia, J. Phys. B **20**, 3737 (1987).
[31] The plotted values (denoted by triangles in Fig. 4) were extracted from the experiments of Refs. [18,19] extrapolating the result for antiprotons and interpolating the results for protons, obtaining the values 0.22 and 0.083, respectively.
[32] A.F. Lifschitz and N.R. Arista, Phys. Rev. A **58**, 2168 (1998), Fig. 2.